JOURNAL OF CATALYSIS 147, 578–593 (1994)

Catalytic Performance and Mechanism for Oxygenated Compound Formation for Ethylene Hydroformylation over Supported Ru–*M* Bimetallic Carbonyl Cluster-Derived Catalysts

Feng-Shou Xiao*,†,[1] and Masaru Ichikawa†

*Department of Chemistry, Jilin University, Changchun 130023, China; and †Catalysis Research Center, Hokkaido University, Sapporo 060, Japan

Received December 7, 1993; revised January 25, 1994

The catalytic performance in ethylene hydroformylation over SiO_2, MgO, and carbon-supported Ru, Ru–Co, Ru–Mn, Ru–Cr, and Co carbonyl cluster-derived catalysts has been investigated, and it was found that the catalysts derived from Ru monometallic and Ru–Co bimetallic carbonyl clusters are active in ethylene hydroformylation. The presence of Co atoms in Ru–Co carbonyl clusters led to a remarkable increase in the rate of product formation, especially for oxygenates. The Ru–Mn bimetallic carbonyl cluster-derived catalyst showed similar conversion, but it exhibited poor activity and selectivity for oxygenates as compared with catalysts derived from $Ru_6C(CO)_{17}$. In contrast to the $Ru_6C(CO)_{17}$ carbonyl cluster-derived catalyst, the Ru–Cr bimetallic carbonyl cluster-derived catalyst exhibited very low activity and selectivity for ethane and oxygenates, indicating that the Cr sites in Ru–Cr bimetallic carbonyl cluster-derived catalyst have a poisoning effect on ethylene hydroformylation. The nature of support has been shown to have a large influence on the catalytic activity and selectivity of the resulting catalyst. The effect of Co promotion in Ru–Co carbonyl clusters on silica and carbon was much stronger than that on MgO. The nature of these Ru–Co/SiO_2 catalyts has been investigated by infrared and X-ray photoelectron spectroscopes. The IR spectra of CO on reduced Ru–Co/SiO_2 catalysts prepared from Ru–Co bimetallic carbonyl clusters exhibited bands at 1684 cm^{-1}. The reaction of CO and H_2 with Ru–Co/SiO_2 catalysts showed a band at 1584 cm^{-1}. *In situ* IR spectra of the reaction of CO + H_2 + C_2H_4 on these reduced Ru–Co/SiO_2 catalysts exhibited bands at 1585 and 1555 cm^{-1} shifting to 1540 and 1520 cm^{-1} by ^{13}CO isotopic effect, which are strongly related to the activity and selectivity for propanol and propaldehyde in ethylene hydroformylation.

INTRODUCTION

The use of metal carbonyl clusters as a catalyst precursor is an important aspect of homogeneous and heterogeneous catalysis (1–5). Attractive features of such catalyst preparation include very high metal dispersion and well-defined metal composition. Furthermore, the bimetallic clusters offer prospects of synergistic effect for the two metal components in many useful catalytic reactions. Recently, bimetallic clusters grafted on solid surfaces have attracted much attention because they may provide highly dispersed bimetallic particles (6–8). These catalysts exhibit good catalytic performance in many catalytic reactions such as CO hydrogenation and olefin hydroformylation when compared with the conventional catalysts prepared by co-impregnation and ion exchange of metal salts (1, 5–9). Catalytic, electronic, and structural properties of the bimetallic catalysts are associated with the composition of the metal component, geometric situation of bimetallic species and the nature of the support (1–10).

In CO hydrogenation on salt-derived Rh/SiO_2 and Pd/SiO_2 catalysts, some additive metal ions such as Mn, Ti, Zr, and Fe promote the production of oxygenates including aldehydes, alcohols, and acetic acid (9, 11–14), and the mechanism of hydrocarbon and oxygenate formation has been widely investigated (15–25). These results suggest that the surface carbon formed by the dissociation of CO is an intermediate for hydrocarbon formation (15–19) and that the formation of oxygenates involves the insertion of CO into adsorbed species such as methyl and carbene (20–24). Several intermediates for forming oxygenates have been proposed, such as acetate (20–22), acetyl (21, 22), formate (24–28), and formyl (9, 29–33).

The hydroformylation of ethylene with syngas has been used as a probe reaction for investigating the mechanism and activity of the CO hydrogenation over some catalysts for catalyzing the specific reaction steps (34–37). The added ethylene in CO + H_2 may undergo various specific reactions: (i) hydrogenation and (ii) CO insertion lead to the formation of ethane and propaldehyde, respectively.

In the homogeneous olefin hydroformylation reaction, ruthenium carbonyls exhibit poor activity even under high pressure conditions, compared with cobalt or rhodium

[1] To whom correspondence should be addressed. Permanent address: Department of Chemistry, Jilin University, Changchun 130023, China. Present address: Department of Chemical Engineering, University of California, Davis, CA 95616.

0021-9517/94 $6.00

carbonyls, but the competitive hydrogenation of olefin to paraffin occurs preferentially (38). It was previously reported that the mixture of $Co_2(CO)_8/Ru_3(CO)_{12}$ shows synergistic rate enhancement in homogeneous hydroformylation (39, 40). Recently, a series of mixed bimetallic Ru–*M* (*M* = Co, Fe, Mo, Rh, Cr, and Mn) carbonyl cluster-derived catalysts have been investigated (9, 29–33).

In the present study, we prepared a series of mixed-ruthenium bimetallic catalysts using supports such as carbon, MgO, and SiO_2 impregnated with a series of mixed-ruthenium bimetallic carbonyl clusters such as Ru–Co, Ru–*M*, and Ru–Cr bimetallic carbonyl clusters, and we studied the activity and selectivity in hydroformylation of ethylene. Furthermore, we compared the catalytic performance in hydroformylation of ethylene over the catalysts deposited on various supports, and discussed the nature of the various supports. The mechanism of formation of oxygenates from the hydroformylation of ethylene over SiO_2-supported Ru–Co carbonyl cluster-derived catalyst was studied through reaction kinetics, infrared spectra of adsorbed species, and X-ray photoelectron spectroscopy. The origin of Co promotion on the SiO_2-supported Ru–Co bimetallic carbonyl cluster-derived catalysts is discussed.

EXPERIMENTAL

Materials and Catalyst Preparation

Various gases such as H_2, CO, O_2, N_2, C_2H_4, and CO + H_2, with purity > 99.999%, were supplied by Takachiho Trading Co. Isotopic labeled gases of ^{13}CO and D_2 (purity 99.3%) were purchased from MDS isotopes. The aldehydes, alcohols, and acetone were purified by outgassing and vacuum distillation from a dry ice–methanol cold trap to liquid nitrogen cold trap. Aerosil 300 (Nippon Aerosil Co.), silica–alumina catalyst (Davision, Grade 13), and MgO (Merck, GR) were used as supports of SiO_2, SiO_2–Al_2O_3, and MgO, respectively.

All manipulations were performed in an inert atmosphere by the use of a glove box for catalyst preparation. Clusters such as $[Et_4N][HRu_3(CO)_{11}]$ (42), $H_3Ru_3Co(CO)_{12}$ (43, 44), $[Et_4N][Ru_3(CO)_9(CCO)]$ (45), $HRu_3Co(CO)_{12}$ (43, 44), $[Et_4N][MnRu_3C(CO)_{13}]$ (40), $Ru_7C(CO)_{17}$ (40), $Co_3Ru_3C(CO)_{15}$ (40), and $[Et_4N][Cr_2Ru_3C(CO)_{16}]$ (40) were synthesized according to the literature. Each cluter-derived catalyst was prepared by impregnation of the support with a solution of cluster in dry acetone. Each catalyst contained about 3 wt.% Ru for IR characterization and XPS study and 1 wt.% Ru for ethylene hydroformylation. The Ru content was controlled by the use of the appropriate amount of the cluster in the slurry. Prior to use, the support was pretreated in flowing oxygen at 573 K overnight and then evacuated at 573 K for 2 h. In a typical run, 140 mg (or 48 mg) of $H_3Ru_3Co(CO)_{12}$ in 200 ml of acetone was brought in contact with 1 g of silica. After being stirred for 2 h the solvent was evaporated from the slurry under vacuum. The solid was oxidized in an oxygen flow (1×10^5 Pa, 40 ml/min) at 423 K for 2 h in a glass tube, followed by reduction in a hydrogen flow (1×10^5 Pa 40 ml/min) at the programmed temperatures from 293 to 573 K for 2 h and at 573 K for 2 h. Table 1 shows the parameters for the preparing all catalysts used in this work.

Hydroformylation of Ethylene

The ethylene hydroformylation was carried out using an open-flow mode reaction at 345–473 K. A gas mixture of ethylene, CO, and H_2 (1 : 1 : 1 molar ratio at a pressure of 1×10^5 Pa) was passed through the catalyst bed (1 g of catalyst) at a flow rate of 60 ml/min. The oxygenated products such as propanol and propaldehyde were collected by bubbling the effluent gas through a water-filled trap (50 ml of water). The analysis of ethylene was performed by a Shimadzu GC-8AIT gas chromatograph with thermal conductivity detector using a 4 mm × 4 m porapak Q (60–80 mesh) column at 343 K. The concentration of gas products in the off gas was calibrated with an external standard consisting of 5 ml of gas. The analysis of the propanol and propaldehyde dissolved in the water trap was conducted by Shimadzu GC-8APF gas chromatography with a flame ionization detector. Ethanol was added as an internal standard to calibrate the concentration of propanol and propaldehyde. For each gas chromatogram the amount of products was determined with an integrator (CR-6A, Shimadzu).

Infrared Spectroscopy (IR)

Each catalyst (Ru loading 3%) was pressed into a self-supporting disk (15 mm in diameter and 10–12 mg/cm^2 in weight) and the catalyst disk was placed in an infrared quartz cell with CaF_2 windows. After reduction for 2 h at 573 K in an H_2 flow (60 ml/min, 1×10^5 Pa), the sample disk was cooled to 298 K and evacuated for 1 h at 298 K. Then, the reaction gas was introduced into the cell and infrared spectra were measured in the region 4000–1000 cm^{-1} by using a Fourier transform spectrometer (FT-IR 4100, Shimadzu Co.) with a resolution of 2 cm^{-1}.

X-Ray Photoelectron Spectroscopy (XPS)

Each cayalyst (Ru loading 3%) was pressed into a self-supporting disk (15 mm in diameter and 30 mg/cm^2 in weight) and placed into the stainless-steel chamber with an upper high vacuum (10^{-6} Pa). The Ru3*d* and Co3*p*

TABLE 1

Preparation of Ru Monometallic and Ru–*M* (*M* = Co, Mn, and Cr) Bimetallic Carbonyl Cluster-Derived Catalysts

Precursors	Ref.	Weight (mg)	Support (g)	Ru loading (%)
$[Et_4N][HRu_3(CO)_{11}]$	42	73 (210)	SiO_2: 3.0	1.0 (3.0)
			Carbon: 3.0	1.0
			MgO: 3.0	1.0
$Ru_6C(CO)_{17}$	40	58 (170)	SiO_2: 2.0	1.0 (3.0)
			Carbon: 2.0	1.0
			MgO: 2.0	1.0
$[Et_4N][HRu_3(CO)_9CCO]$	45	28 (84)	SiO_2: 1.0	1.0 (3.0)
			Carbon: 1.0	1.0
			MgO: 1.0	1.0
$H_3Ru_3Co(CO)_{12}$	43, 44	48 (140)	SiO_2: 2.0	1.0 (3.0)
			Carbon: 2.0	1.0
			MgO: 2.0	1.0
$HRuCo_3(CO)_{12}$	43, 44	61 (180)	SiO_2: 2.0	1.0 (3.0)
			Carbon: 2.0	1.0
			MgO: 2.0	1.0
$Ru_3Co_3C(CO)_{15}$	40	30 (87)	SiO_2: 2.0	1.0 (3.0)
			Carbon: 2.0	1.0
			MgO: 2.0	1.0
$[Et_4N]_2[Ru_3MnC(CO)_{14}]$	40	34	Carbon: 1.0	1.0
$[PPN]_2[Ru_3Cr_2(CO)_{16}]$	40	64	Carbon: 1.0	1.0
$Co_4(CO)_{12}$		25	SiO_2: 1.0	1.0
$[Et_4N][HRu_3(CO)_{11}] + Co_4(CO)_{12}$		73 + 75	SiO_2: 1.0	1.0

spectra were measured with a V.G. ESCALAB Mark II system. An Al$K\alpha$ X-ray source ($h\nu$ = 1486.6 eV) was used, and the X-ray was operated at 14 kV and 20 mA. The binding energies were calculated by taking the energy of the 2*P* of silicon atom (104.0 eV) in silica as an internal standard.

RESULTS

Ethylene Hydroformylation

SiO_2-supported cluster-derived catalysts. Catalytic hydroformylation of ethylene over various Ru, Ru–Co, and Co carbonyl cluster-derived catalysts gives products of ethane, propaldehyde, and propanol, and the rates of formation for products vary greatly with reaction time. For all catalysts, initially, a high rate of ethane formation and a low rate of oxygenate formation were found. With an increase in reaction time, the ethane rate decreased remarkably, while oxygenates reduced slightly.

As a typical example, the catalytic activity of the silica-supported $H_3Ru_3Co(CO)_{12}$ bimetallic carbonyl cluster-derived catalyst required about 30 h to reach steady state for ethane and oxygenates in the ethylene hydroformylation reaction at 442 K. In periods of 30 h or more, the reactivity basically remained a constant, which strongly indicates that the catalyst has a long life in ethylene hydroformylation, as shown in Fig. 1.

Activity and selectivity in ethylene hydroformylation at steady state over Ru, Ru–Co, and Co carbonyl cluster-derived catalysts are presented in Table 2, where the specific rates of product formation are expressed as mmol/mol(Ru)min. The Ru_3/SiO_2 catalyst prepared from an anion cluster $[HRu_3(CO)_{11}]^-$ provides 0.20% ethylene conversion. The Co_4/SiO_2 catalyst prepared from the $Co_4(CO)_{12}$ cluster is almost inactive for ethylene hydroformylation. On the Ru–Co bimetallic catalyst prepared from $H_3Ru_3Co(CO)_{12}$, the $Ru_3Co_3C(CO)_{15}$ and $HRuCo_3(CO)_{12}$ bimetallic carbonyl clusters, the ethylene conversion, and the rates for propaldehyde and propanol are substantially increased. The selectivity towards propanol formation on the Ru–Co carbonyl cluster-derived catalysts is much higher than that on the other catalysts. Such a higher rate and selectivity towards propanol and propaldehyde on Ru–Co bimetallic cluster-derived catalysts cannot be explained simply by the additional formation of propanol and propaldehyde from the individual Ru and Co atoms without their cooperativity on the silica. It has been reported that atomic Co in ZnO-supported Rh–Co carbonyl clusters markedly enhanced normal isomer selectivity in propylene hydroformylation (46, 47). The above results indicate that atomic Co in the Ru–Co bimetallic cluster-derived catalysts remarkably promotes the conversion and oxygenate formation. To determine the effect of proximity of Ru and Co in the precursor compounds, two Ru–Co catalysts were prepared from $RuCl_3$ + $CoCl_2$ and

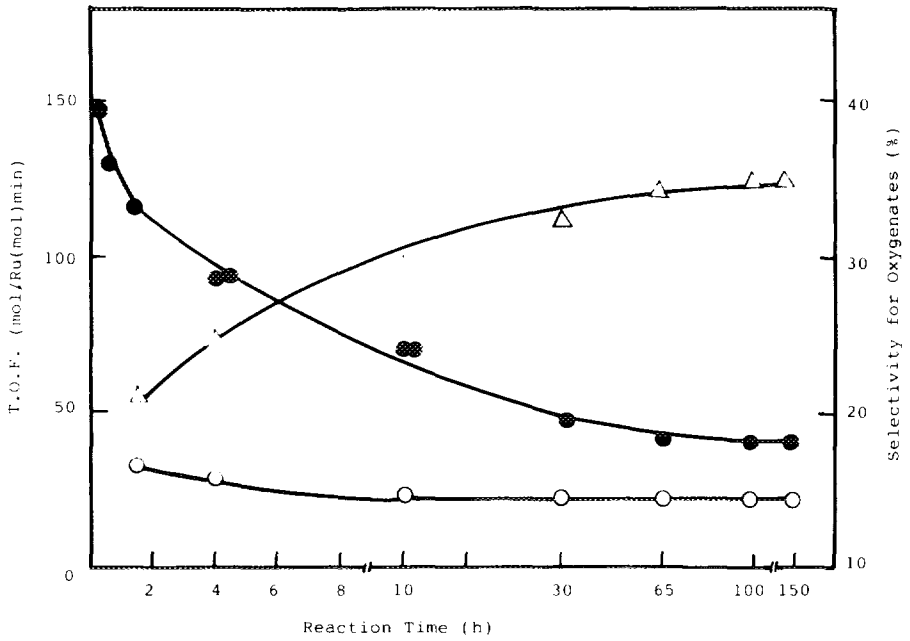

FIG. 1. Rate of formation for oxygenates and ethane as a function of reaction time over silica-supported $H_3Ru_3Co(CO)_{12}$ bimetallic carbonyl cluster-derived catalyst. (●) C_2H_6; (○) oxygenates; (△) selectivity for oxygenates.

from a mixture of monometallic clusters $[HRu_3(CO)_{11}]^-$ and $Co_4(CO)_{12}$ at the Co/Ru molar ratio of 1/3. Both catalysts give higher rates for the products than those for Ru_3/SiO_2 and Co_4/SiO_2 catalysts, but the relative enhancement of the rates is much lower than that on Ru–Co bimetallic carbonyl cluster-derived catalyst.

The temperature dependency of the catalyst was also investigated, and it was observed that the rates of both ethane and oxygenated formation increase with the temperature and that at high temperature ethane predominates.

Carbon-supported cluster-derived catalysts. The results of the atmospheric pressure hydroformylation of ethylene in the vapor phase are presented in Table 3. The Ru_3/SiO_2 catalyst exhibits 0.30% conversion. In comparison with Ru_3/SiO_2, the Ru_6C/SiO_2 catalyst prepared from $Ru_6C(CO)_{17}$ shows high ethylene conversion (0.95%), especially for ethane formation. These results indicate that the carbide contained in $Ru_6C(CO)_{17}$ is an active species for ethylene hydrogenation. In contrast to the catalysts from $[HRu_3(CO)_{11}]^-$ and $Ru_6C(CO)_{17}$, the catalysts from mixed-ruthenium bimetallic clusters impregnated on car-

TABLE 2

Catalytic Performance in Hydroformylation of Ethylene over Silica-Supported Ru, Ru–Co, and Co Carbonyl Cluster-Derived Catalysts

Precursor	Ethylene conv. (%)	Rate of formation ($mmol/mol_{Ru}$ min)		Sel. for oxygenates (%)[a]	Sel. for alcohol (%)[b]
		C_2H_6	$C_2H_5CHO + C_3H_7OH$		
$[Et_4N][HRu_3(CO)_{11}]$	0.20	14	2.9	17	—
$Ru_6C(CO)_{17}$	0.71	52	11	17	6.0
$H_3Ru_3Co(CO)_{12}$	3.7	280	45	14	27
$Ru_3Co_3C(CO)_{15}$	5.4	420	58	12	35
$HRuCo_3(CO)_{12}$	12	980	110	10	27
$Co_4(CO)_{12}$		—	—	—	—
$[Et_4N][HRu_3(CO)_{11}] + Co_4(CO)_{12}$	0.85	62	12	16	4.0
SiO_2		—	—	—	—

[a] $(C_2H_5CHO + C_3H_7OH)/(C_2H_6 + C_2H_5CHO + C_3H_7OH)$ 100%.
[b] $C_3H_7OH/(C_2H_5CHO + C_3H_7OH)$ 100%.

TABLE 3

Catalyatic Performance in Hydroformylation of Ethylene over Carbon-Supported Ru, Ru–Co, and Co Carbonyl Cluster-Derived Catalysts

Precursor	Ethylene conv. (%)	Rate of formation ($mmol/mol_{Ru}$ min)		Sel. for oxygenates (%)[a]	Sel. for alcohol (%)[b]
		C_2H_6	$C_3H_5CHO + C_3H_7OH$		
$[Et_4N][HRu_3(CO)_{11}]$	0.30	24	3.0	11	—
$Ru_6C(CO)_{17}$	0.95	73	12	14	12
$H_3Ru_3Co(CO)_{12}$	3.5	270	37	12	10
$Ru_3Co_3C(CO)_{15}$	5.5	440	51	10	27
$HRuCo_3(CO)_{12}$	14	1100	130	10	47

[a] $(C_2H_5CHO + C_3H_7OH)/(C_2H_6 + C_2H_5CHO + C_3H_7OH)$ 100%.
[b] $C_3H_7OH/(C_2H_5CHO + C_3H_7OH)$ 100%.

bon exhibit the following features: (i) The rate of ethylene hydrogenation is greatly increased. As a result, the selectivity for oxygenates is very low. (ii) The rates of ethane and oxygenates in ethylene hydroformylation over Ru–Co cluster-derived catalysts are very high, especially for the formation of propanol and propaldehyde. A plot of TOF for ethylene hydroformylation vs Co/Ru ratio shows a smooth cruve (Fig. 2), with an increase in TOF of oxygenate formation as the Co content increases being observed. (iii) The activity of the Cr_2Ru_3C/SiO_2 catalyst is remarkably low, and the TOFs are in fact much lower than those for the nonpromoted Ru_6C/SiO_2 catalyst. This indicates that the Cr has some poisoning effect on the catalyst.

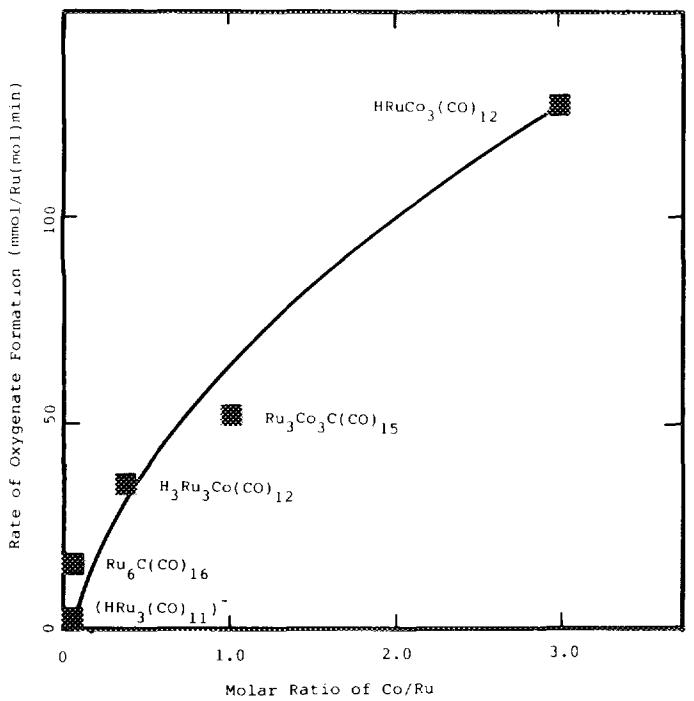

FIG. 2. Plot of rate of formation vs molar ratio of Co/Ru carbon-supported Co–Ru bimetallic carbonyl cluster-derived catalyst.

MgO-supported cluster-derived catalysts. The results of ethylene hydroformylation over various cluster-derived catalysts are summarized in Table 4, and we observed that the activity on a series of Ru–Co cluster-derived catalysts is higher than that on Ru_3SiO_2 and Co_4/SiO_2 catalysts.

By comparing Tables 2–4, we find the following features: (i) The cobalt promotion in the Ru–Co bimetallic cluster-derived catalysts on MgO is much lower than those on silica and carbon. For example, the rate of oxygenated formation for Ru_3Co/MgO catalyst is only two times that for Ru_3/MgO, but the rates of oxygenate formation for the Ru_3Co/SiO_2 and Ru_3Co/carbon catalysts are as high as 15 and 12 times those for Ru_3/SiO_2 and Ru_3/carbon. (ii) Ethylene conversion over MgO-supported cluster-derived catalysts is very low in comparison with that over silica and carbon-supported cluster-derived catalysts. (iii) The selectivities for oxygenates and propanol on MgO-supported cluster-derived catalysts are much higher than those on silica and carbon-supported cluster-derived catalysts. The above features may be influenced by the nature of supports.

Infrared Spectra

It was observed that the carbon- and silica-supported Ru–Co bimetallic carbonyl cluster-derived catalysts exhibit higher activity and selectivity for oxygenates in ethylene hydroformylation than those on MgO-supported Ru–Co bimetallic carbonyl cluster-derived catalysts, but it is difficult to pass the IR beam through carbon-supported catalysts. We therefore selected the silica-supported catalysts for the IR studies.

CO chemisorption. Figure 3 shows the IR spectra in the carbonyl region for the Ru_6C/SiO_2 catalyst derived from the $Ru_6C(CO)_{17}$ cluster. When a freshly reduced sample at 298 K is exposed to 100 Torr CO, the two CO chemisorbed IR bands appear at 2048 cm^{-1} (sharp) and

TABLE 4

Catalytic Performance in Hydroformylation of Ethylene over MgO-Supported Ru, Ru–Co, and Co Carbonyl Cluster-Derived Catalysts

Precursor	Ethylene conv. (%)	Rate of formation (mmol/mol$_{Ru}$ min)		Sel. for oxygenates (%)[a]	Sel. for alcohol (%)[b]
		C_2H_6	$C_3H_5CHO + C_3H_7OH$		
$[Et_4N][HRu_3(CO)_{11}]$	0.15	3.0	10	77	46
$[Et_4N]_2[Ru_3(CO)_9CCO]$	0.46	30	11	27	46
$H_3Ru_3Co(CO)_{12}$	0.52	25	21	46	51
$HRuCo_3(CO)_{12}$	0.62	29	26	47	54
MgO	0.078	2.0	5.0	71	—

[a] $(C_2H_5CHO + C_3H_7OH)/(C_2H_6 + C_2H_5CHO + C_3H_7OH)$ 100%.
[b] $C_3H_7OH/(C_2H_5CHO + C_3H_7OH)$ 100%.

1880 cm^{-1} (broad) in Fig. 3a. These are attributed to terminal and bridged CO on ruthenium surface (48, 49). After evacuation for 20 min at 443 K, the sample exhibits a very weak band at 2084 cm^{-1} and a strong band at 2048 cm^{-1}, with a broad band at 1880 cm^{-1}.

The IR spectra of CO adsorbed on the reduced Ru_3Co_3/SiO_2 catalyst are shown in Fig. 4. At room temperature, bands are observed at 2072, 2036, 2000, 1880, and 1684 cm^{-1}. The bands at 2072, 2036, and 2000 cm^{-1} are generally assigned to linear CO chemisorbed on Ru sites, and the broad and weak band at 1880 cm^{-1} is assigned to the bridge CO chemisorption on Ru sites (48,49). In contrast to Ru_6/SiO_2 catalyst, the frequencies of linear CO ad-

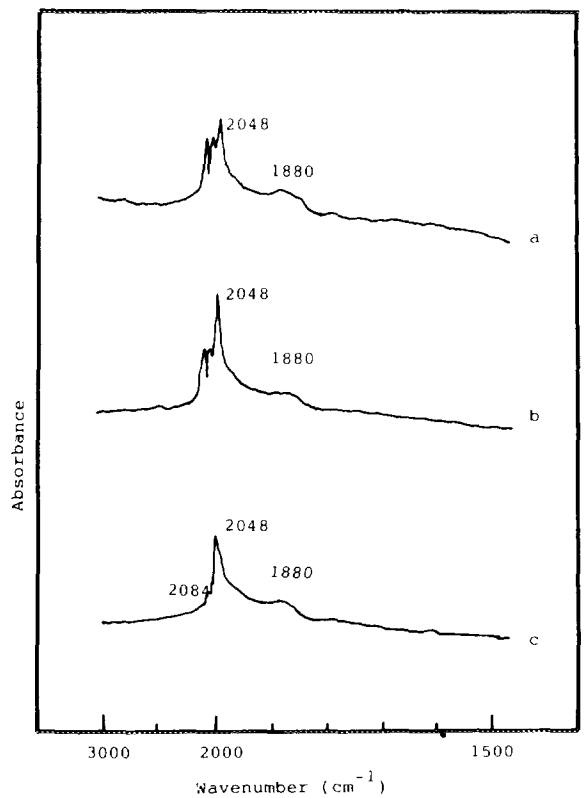

FIG. 3. IR spectra in CO adsorption at 298–443 K on the silica-supported reduced $Ru_6C(CO)_{17}$ carbonyl cluster-derived catalyst (reduction for 4 h at 573 K). (a) Adsorption of 100 Torr CO for 1 h at 298 K; (b) after (a), adsorption for 1 h at 443 K; (c) after (b), evacuation for 20 min at 443 K.

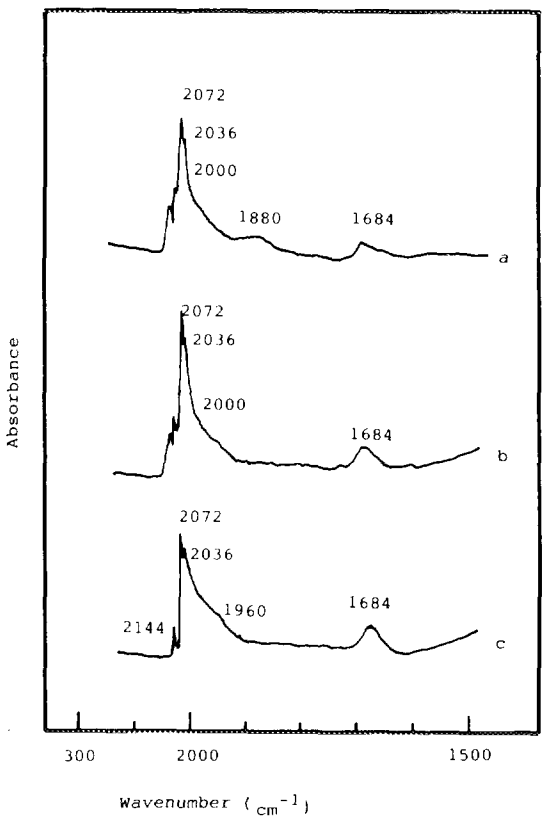

FIG. 4. IR spectra in CO adsorption at 298–443 K on the silica-supported reduced $Ru_3Co_3(CO)_{15}$ carbonyl cluster-derived catalyst (reduction for 4 h at 573 K). (a) Adsorption of 100 Torr CO for 1 h at 298 K; (b) after (a), adsorption for 1 h at 443 K; (c) after (b), evacuation for 20 min at 443 K.

sorbed on Ru_3Co_3/SiO_2 catalyst shift to higher wavenumbers, which may be due to the *d-electron* transference from Ru to Co sites. This phenomenon was also observed for Ru–Co–Mo/Al_2O_3 catalyst (50–52).

Of special interest is the band at 1684 cm^{-1}, which shifts to 1640 cm^{-1} with ^{13}CO on the Ru_3Co_3/SiO_2 catalyst due to ^{13}CO isotopic effect. Ichikawa and co-workers (12, 13, 50, 51) and Hoffman and Depola (52) have reported that the conventional Rh–Mn, Rh–Ti, Rh–Zr, and Rh–Fe/SiO_2 catalysts are very active for oxygenate formation in CO hydrogenation, and that these catalysts display a large reduction of the CO frequency (1730–1580 cm^{-1}). Horwiz and Shriver (53) reported that the stoichiometric formation of adducts between metal carbonyls such as $Fe_2(CO)_9$ and $Ru_3(CO)_{12}$ and Lewis acids such as $AlCl_3$, BF_3, and Al_2O_3 arises from C- and O-bound CO, characteristic of bands at 1740–1520 cm^{-1}. It is therfore suggested that the Ru–Co sites in the catalyst give two-site CO activation, where the carbon of chemisorbed CO is bonded to two Ru sites and its oxygen atom to promoter metal ions, as previously reported by Xiao *et al.* (9).

When the sample disk is heated to 443 K for 1 h, the band at 1880 cm^{-1} almost disappears, and the intensity of the band at 1684 cm^{-1} increases. This may mean that the species of CO bridge adsorption transfer to 1684 cm^{-1} species.

Adsorption of CO and H_2. The spectra of CO and H_2 on the Ru_6/SiO_2 and Ru_3Co_3/SiO_2 catalysts are shown in Fig. 5. The spectrum for Ru_6/SiO_2 catalyst exhibits broad bands at 2048 and 1880 cm^{-1} and weak bands at 2932 and 2860 cm^{-1}, which are assigned to CO and CH stretching frequencies, respectively (48, 49, 54). On the other hand, for the Ru_3Co_3/SiO_2 catalyst, it is very interesting that, in addition to the bands at 2930, 2860, 2060, and 1880 cm^{-1}, a band at 1584 cm^{-1} is observed, which has a linear relationship to the activity and selectivity for oxygenate formation in CO hydrogenation, and is likely assigned to formyl species, as discussed by Xiao and co-workers (9, 29–33).

Adsorption of alcohols and aldehydes. Since the C_3+ alcohol and aldehyde are products of ethylene hydroformylation on these catalysts, we employed them as probe molecules on the surface of Ru_6/SiO_2 and Ru_3Co_3/SiO_2 catalysts.

After the Ru_6/SiO_2 catalyst was reduced for 4 h at 673

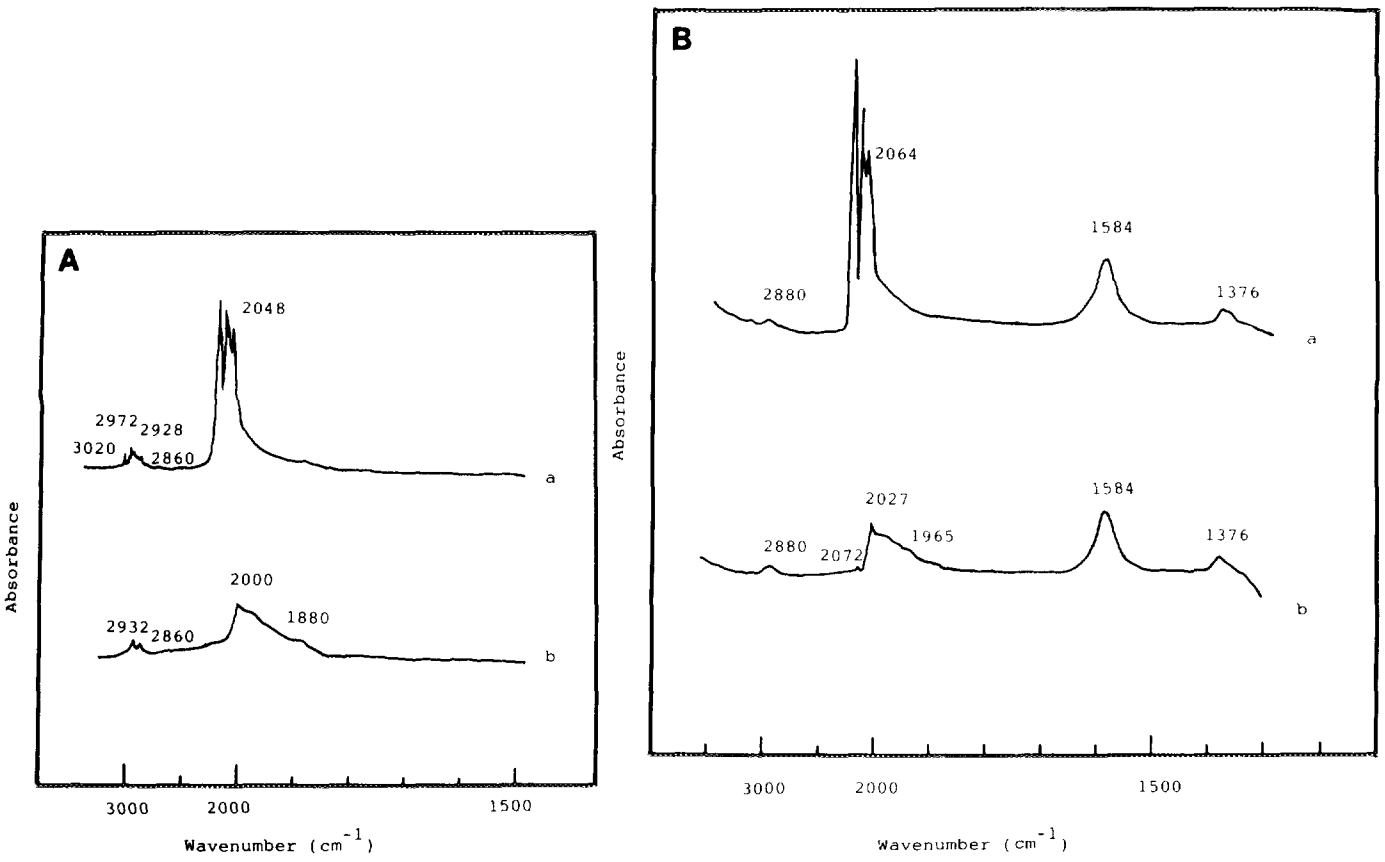

FIG. 5. IR spectra of the silica-supported catalyst after reaction with CO and H_2: (A) $Ru_6C(CO)_{17}$ and (B) $Ru_3Co_3C(CO)_{15}$ carbonyl cluster-derived catalyst reduced for 4 h at 573 K (reaction flow: H_2/CO = 1/1, total 40 ml/min; reduction flow: H_2 40 ml/min). (a) The reaction for 2 h at 443 K; (b) after (a), evacuation for 20 min at 443 K.

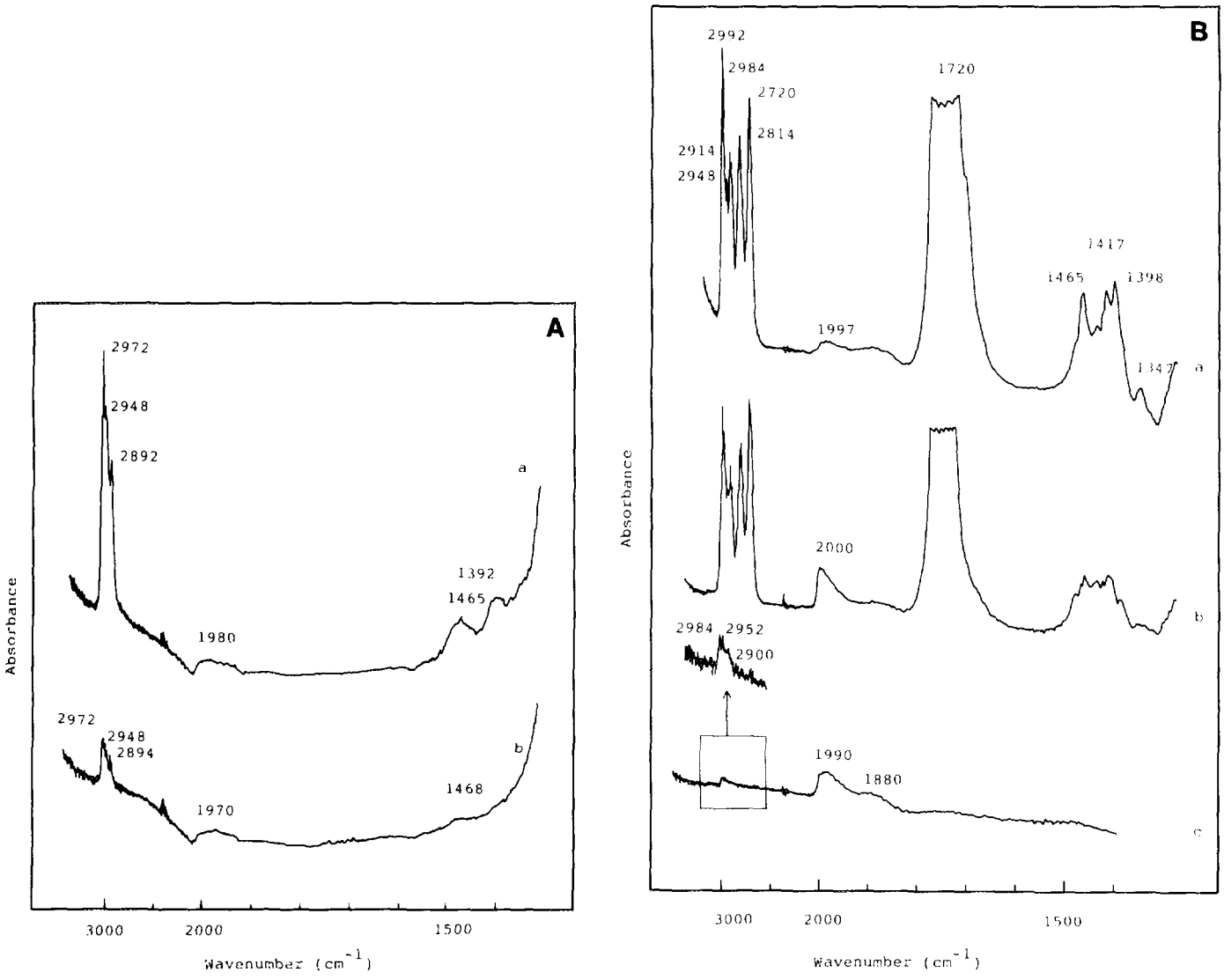

FIG. 6. IR spectra of (A) $C_2H_5CH_2OH$ and (B) C_2H_5CHO adsorbed on silica-supported reduced $Ru_6C(CO)_{17}$ carbonyl cluster-derived catalyst reduced for 4 h at 573 K. (a) Adsorption for 1 h at 443 K; (b) after (a), evacuation for 20 min at 443 K.

K and evacuated for 1 h at the same temperature, 20 Torr C_3H_7OH was admitted into a quartz cell. As shown in Fig. 6A, the sample spectrum shows the bands at 2972, 2948, and 2892 cm^{-1} at 1465 and 1392 cm^{-1}, and at 1980 cm^{-1}. The bands at 2972, 2948, and 2894 cm^{-1} and at 1465 and 1392 cm^{-1} are reasonably assigned to the C–H stretching and deformation modes of CH_3 and CH_2 species (54–56). The 1980 cm^{-1} band is assigned to linear CO adsorption, resulting from the dehydrogenation of propanol. After evacuation for 20 min, the bands assigned to CH_3 and CH_2 species decreased remarkably. As shown in Fig. 6B, the adsorption of propaldehyde on Ru_6/SiO_2 gives many bands. The bands at 2992, 2984, 2948, 2914, 2814, and 2720 cm^{-1}, and at 1465, 1417, 1398, and 1347 cm^{-1} are also assigned to C–H stretching and deformation frequencies of CH_3, CH_2, and CH species. The very strong band near 1720 cm^{-1} is attributed to the carbonyl frequency of the CHO group.

On the other hand, as shown in Fig. 7, the IR spectrum of propanol and propaldehyde adsorbed on the Ru_3Co_3/SiO_2 catalyst exhibits a new band at 1550–1555 cm^{-1}, in addition to the bands assigned to C–H stretching and deformation modes, as compared with those on Ru_6/SiO_2 catalyst.

Furthermore, we carried out the adsorption of CH_3CDO on reduced Ru_3Co_3/SiO_2 catalyst. For CH_3CDO gas phase, the C–H stretching and deformation frequencies appear at 2960 and 1450 cm^{-1}, and the C–D asymmetric and symmetric frequencies appear at 2072 and 2048 cm^{-1}. The carbonyl frequency of CDO should occur at around 1700 cm^{-1}, as shown in Fig. 8a. Following evacuation for 20 min at 443 K to remove gaseous phase and weak

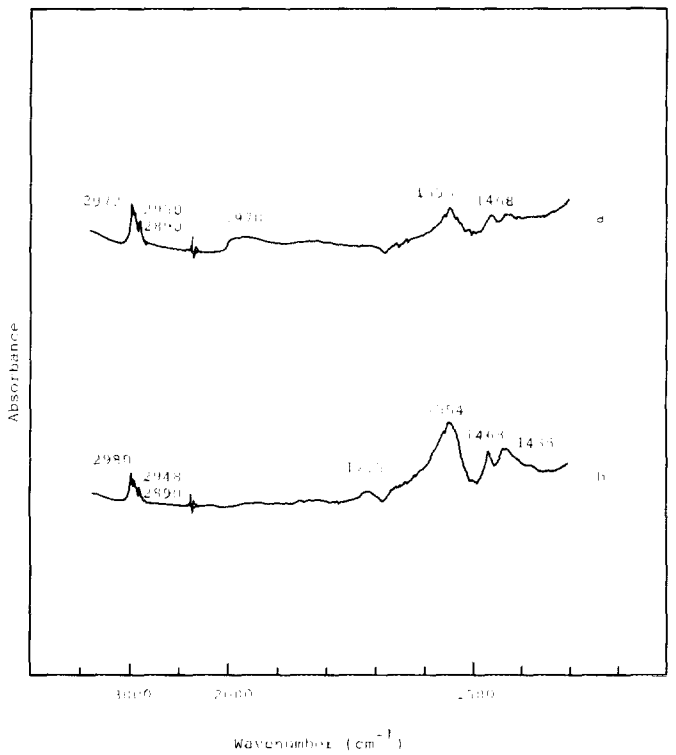

FIG. 7. IR spectra of (a) $C_2H_5CH_2OH$ and (b) C_2H_5CHO adsorbed on silica-supported reduced $Ru_3Co_3(CO)_{15}$ carbonyl cluster-derived catalyst (reduction for 4 h at 573 K) for 1 h at 443 K and evacuation for 20 min at 443 K.

chemisorbed species, the spectrum of the sample contains bands at 2960, 1557, 1449, and 1382 cm^{-1} plus a broad band at 1940 cm^{-1}. We do not observe the bands at 2072 and 2048 cm^{-1} assigned to characteristic C–D vibration. This indicates the lack of C–D species on the surface of the Ru_3Co_3/SiO_2 catalyst.

IR spectra of ethylene, CO, and H_2. IR spectra of ethylene, CO, and H_2 on Ru_6/SiO_2 and Ru_3Co_3/SiO_2 catalysts are shown in Figs. 9 and 10, respectively. Gaseous ethylene bands appear at 3124, 3078, 3020, 2988, 2958, and 2970 cm^{-1}, at 1914, 1888, and 1866 cm^{-1}, and at 1465, 1445, and 1418 cm^{-1}, which are assigned to C–H stretching, C=C stretching, and C–H deformation modes, respectively. Reaction of ethylene, CO, and hydrogen for 4 h at 443 K over Ru_6/SiO_2 catalyst gives a band around 2034 cm^{-1}. After evacuation for 20 min at 443 K to remove the gas phase, the sample spectrum exhibits a broad band at 1980 cm^{-1}, with very weak bands at 2960, 2928, and 2850 cm^{-1}, as shown in Fig. 9.

By contrast, Fig. 10A shows that, in addition to the bands at 2028 and 1999 cm^{-1} assigned to linear CO adsorption, there are new bands at 1584 and 1555 cm^{-1} for the Ru_3Co_3/SiO_2 catalyst. After evacuation for 20 min at 443 K, the sample spectrum gives bands at 2144, 2070, 2000, 1971, 1584, and 1555 cm^{-1}, and very weak bands at 2960, 2880, and 1433 cm^{-1}, as shown in Fig. 10B. Furthermore, with an increase of reaction time, as given in Fig. 11A, the intensity of the 1999 cm^{-1} band decreases remarkably, while the bands at 1584 cm^{-1} and 1555 cm^{-1} increase significantly. The bands assigned to the bridged CO adsorption overlap with the characteristic ethylene bands. We therefore cannot observe the change in bridging CO on Ru sites. Additionally, we were interested in the change of the 1584 and 1555 cm^{-1} bands. After increasing the reaction temperature to 443 K, the IR spectra show both 1584 and 1555 cm^{-1} bands, where the 1584 cm^{-1} species is still predominant. Upon holding this temperature for 30 h, the intensity of the 1555 cm^{-1} band becomes greater than that of the 1584 cm^{-1} band. It seems that the 1584 cm^{-1} species can be easily converted into the 1555 cm^{-1} species by the reaction with surface group. The relationship between the absorbance of IR bands at 1555 and 1584 cm^{-1} and reaction time over Ru_3Co_3/SiO_2 catalyst is shown in Fig. 11B.

We then studied the IR spectra of reaction gases on silica-supported $H_3Ru_3Co(CO)_{12}$, and $HRuCo_3(CO)_{12}$ cluster-derived catalysts. We again observe bands at 1584 and 1555 cm^{-1}, as shown in Fig. 12. Table 5 summarizes the intensities of the IR bands and rate of oxygenated formation on various Ru–Co bimetallic catalysts. A good

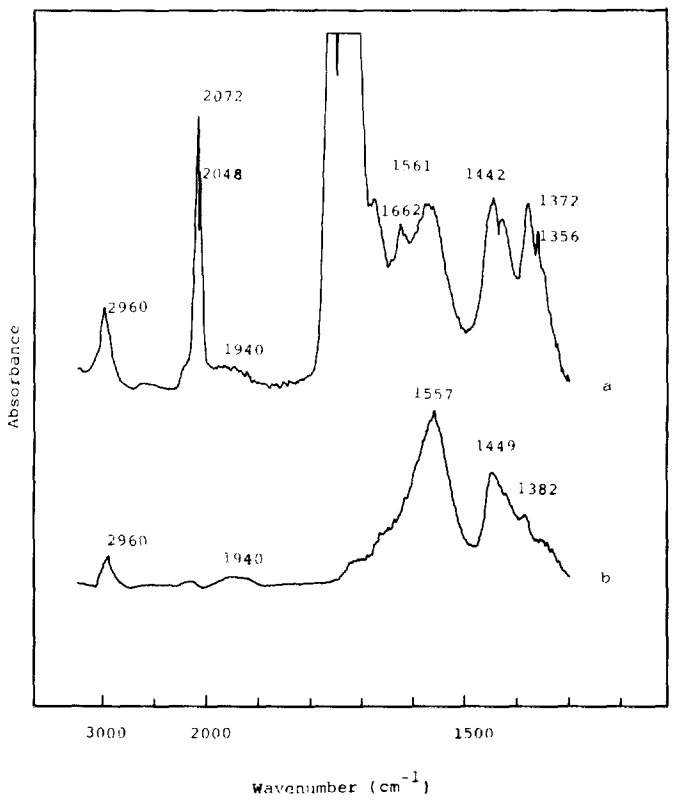

FIG. 8. IR spectra of adsorption of CH_3CDO on silica-supported reduced $Ru_3Co_3(CO)_{15}$ carbonyl cluster-derived catalyst (reduction for 4 h at 573 K). (a) Adsorption for 1 h at 443 K; (b) after (a), evacuation for 20 min at 443 K.

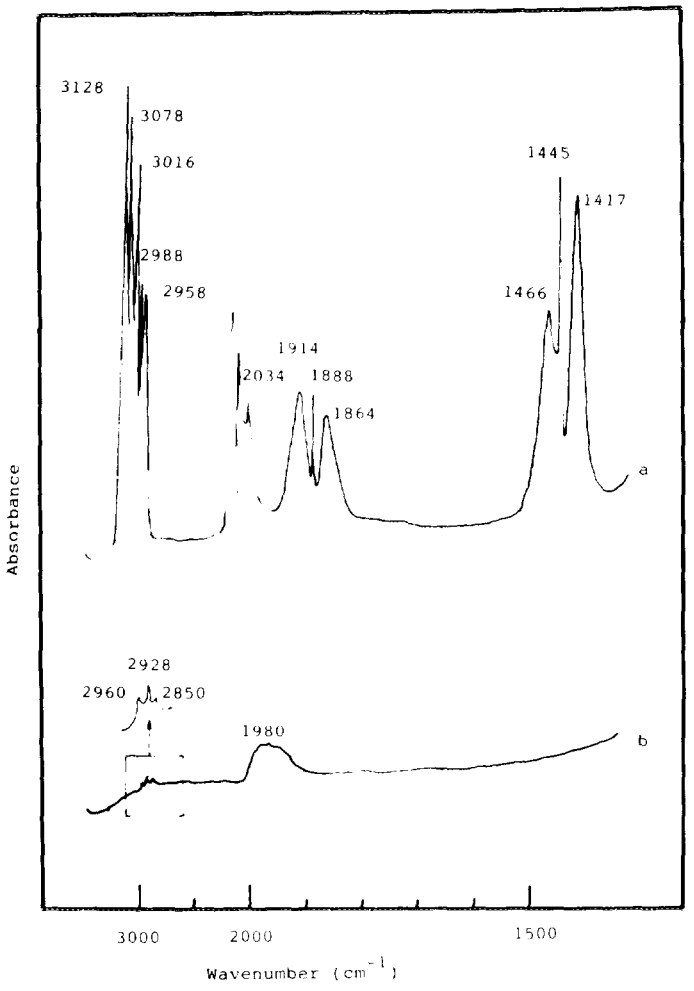

FIG. 9. IR spectra of the catalyst after reaction with CO, H_2, and C_2H_4 on silica-supported reduced $Ru_6C(CO)_{17}$ carbonyl cluster-derived catalyst reduced for 4 h at 573 K (reaction flow: $H_2/CO/C_2H_4$ = 1/1/1, total 60 ml/min; reduction flow: H_2 40 ml/min). (a) The reaction for 2 h at 443 K; (b) after (a), evacuation for 20 min at 443 K.

linear relationship is observed between the 1584 and 1555 cm^{-1} bands and the rate of oxygenate formation, which implies the two species are very important for the formation of propaldehyde and propanol.

X-Ray Photoelectron Spectroscopy

The Co2*p* and Ru3*d* spectra of the fresh, reduced, and used $RuCo_3/SiO_2$ catalysts were recorded by X-ray photoelectron spectroscopy, as shown in Fig. 13. For the fresh catalyst, $Co2p_{1/2}$ and $Co2p_{3/2}$ spectra exhibit peaks at 796.8 and 780.8 eV, and the $Ru3d_{5/2}$ spectrum shows a very weak shoulder peak at 282.6 eV due to the overlap of C1*s* and Ru3*d*. These are in good agreement with spectra taken on CoO and ruthenium oxides (57–60). After reaction of the catalyst for 2 h at 573 K, the peak at 280.3 eV ($Ru3d_{5/2}$) with higher intensity shifted from 282.6 eV is observed. By contrast, the Co3*p* spectra basically keep

TABLE 5

The Intensities (Absorbance) of Infrared Bands at 2000, 1584, and 1555 cm^{-1} and Rates of Oxygenate Formation in Ethylene Hydroformylation over Ru and Ru–Co Carbonyl Cluster-Derived Catalysts

Precursor	Band intensity[a] 2000[c]	1584[c]	1555[d]	TOF of oxygenates[b] ($mmol/mol_{Ru}$ min)
$[Et_4N][HRu_3(CO)_{11}]$	0.037	0.000	0.000	2.9
$Ru_6C(CO)_{17}$	0.041	0.000	0.000	11
$H_3Ru_3Co(CO)_{12}$	0.059	0.034	0.030	45
$Ru_3Co_3C(CO)_{15}$	0.077	0.052	0.049	58
$HRuCo_3(CO)_{12}$	0.14	0.13	0.11	110

[a] $CO/H_2/C_2H_4$ = 1/1/1, total 60 ml/min, 1 × 10^5 Pa.
[b] $CO/H_2/C_2H_4$ = 1/1/1, total 60 ml/min, 1 × 10^5 Pa, 443 K.
[c] Reaction for 3 h at 443 K.
[d] Reaction for 30 h at 443 K.

their intensity and position. These results indicate that the reduction by hdyrogen leads to the change of oxidized ruthenium to lower chemical valence, but Co sites remain as Co^{2+}. After reaction of ethylene, CO, and hydrogen with the reduced catalyst for 20 h at 443 K, the peak positions and intensities of Co2*p* and Ru3*d* are the same as those of the reduced catalyst. This demonstrates that the Ru and Co sites on both the reduced and the used catalyst are in the same chemical states (57–60).

Furthermore, the overlapped C1*s* and Ru3*d* spectra were fit by computer, using C1*s* and Ru3*d* spectra, and the data on binding energy and full-width half-maxima (FWHM) are shown in Fig. 14 and Table 6, respectively. For the reduced and the used catalysts, two types of

TABLE 6

The Fitting Results of XPS Treated by Computer over $HRuCo_3(CO)_{12}$ Cluster-Derived Catalyst

$Ru–Co/SiO_2$ Catalyst		Binding energy (eV)	FWHM (eV)
Fresh	$Ru3d_{5/2}$	282.6	2.3
	$Ru3d_{3/2}$	286.8	2.4
	C1*s* (I)	285.5	2.8
	C1*s* (II)	188.2	1.9
	C1*s* (III)	289.7	1.3
Reduced	$Ru3d_{5/2}$ (I)	280.3	2.0
	$Ru3d_{3/2}$ (I)	284.2	2.1
	$Ru3d_{5/2}$ (II)	281.4	2.3
	$Ru3d_{3/2}$ (II)	285.6	2.4
	C1*s* (I)	285.4	2.8
	C1*s* (II)	287.9	1.9
Used	$Ru3d_{5/2}$ (I)	280.2	2.0
	$Ru3d_{3/2}$ (I)	284.2	2.1
	$Ru3d_{5/2}$ (II)	281.3	2.3
	$Ru3d_{3/2}$ (II)	285.6	2.4
	C1*s* (I)	285.4	2.8
	C1*s* (II)	287.6	1.9
	C1*s* (III)	288.7	2.0

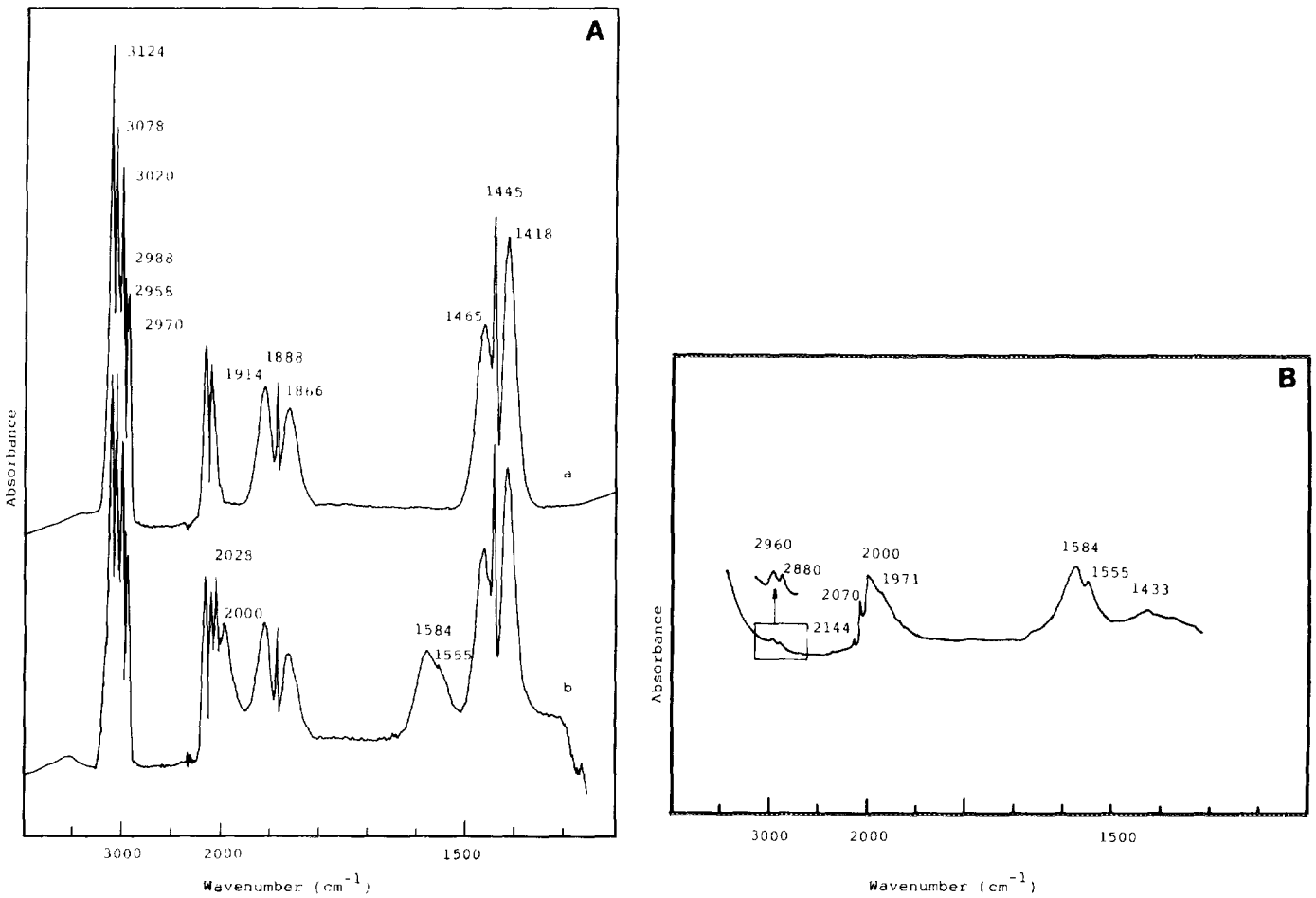

FIG. 10. IR spectra of the catalyst after reaction with CO, H_2, and C_2H_4 on silica-supported reduced $Ru_3Co_3(CO)_{15}$ carbonyl cluster-derived catalyst reduced for 4 h at 573 K (reaction flow: $H_2/CO/C_2H_4$ = 1/1/1, total 60 ml/min; reduction flow: H_2 40 ml/min). (A) (a) Reaction gases; (b) the reaction for 2 h at 443 K. (B) After (b), evacuation for 20 min at 443 K.

ruthenium sites appear at 280.1 and 281.4 eV for Ru3$d_{5/2}$ spectra, which may be assigned to Ru^0 and $Ru^{\delta+}$ (δ = 0–1) species, respectively. Similar results have been reported by Ding (61) and others (62, 63). Additionally, by comparison of the reduced catalyst with the used catalyst, C1s spectra show a peak at 287.6 eV in addition to the bands at 285.4 eV. The new peak for C1s may be assigned to coke and the formation of hydrocarbon groups on the surface.

DISCUSSION

Ethylene Hydroformylation

The large difference in catalytic performance in hydroformylation of ethylene over SiO_2-, carbon-, and MgO-supported catalysts impregnated from $[HRu_3(CO)_{11}]^-$, $Ru_6C(CO)_{17}$, $Co_4(CO)_{12}$, and series of Ru–Co bimetallic carbonyl clusters, $[MnRu_3C(CO)_{14}]^{2-}$ and $[Cr_2Ru_3C(CO)_{16}]^{2-}$, as well as the impregnation of $[HRu_3(CO)_{11}]^-$ + $Co_4(CO)_{12}$ and $RuCl_3$ + $CoCl_2$ are displayed in Tables 2–4. It is interesting to see that both the hydroformylation to propaldehyde and propanol and the simple hydrogenation to ethane are markedly enhanced on the catalysts derived from a series of Ru–Co bimetallic carbonyl clusters, as compared with the catalysts derived from $[HRu_3(CO)_{11}]^-$, $Ru_6C(CO)_{17}$, and $Co_4(CO)_{12}$, and even physical mixtures of $[HRu_3(CO)_{11}]^-$ + $Co_4(CO)_{12}$ and $RuCl_3$ + $CoCl_2$. Moreover, the selectivity towards propanol increases with increasing Co/Ru in the Ru–Co bimetallic carbonyl clusters. The large difference in ethylene hydroformylation could be due to variation in the surface structure and active sites, which are related to changes in metal loading, metal dispersion, surface area, and other preparation conditions. We know that the Ru loading and the other preparation conditions of various Ru and Ru–Co bimetallic catalysts are the same, and the surface areas of these catalysts, as determined by the BET method, are very similar. Therefore, the large difference in catalytic activity and selectivity between Ru_3/SiO_2, Co_4/SiO_2 cata-

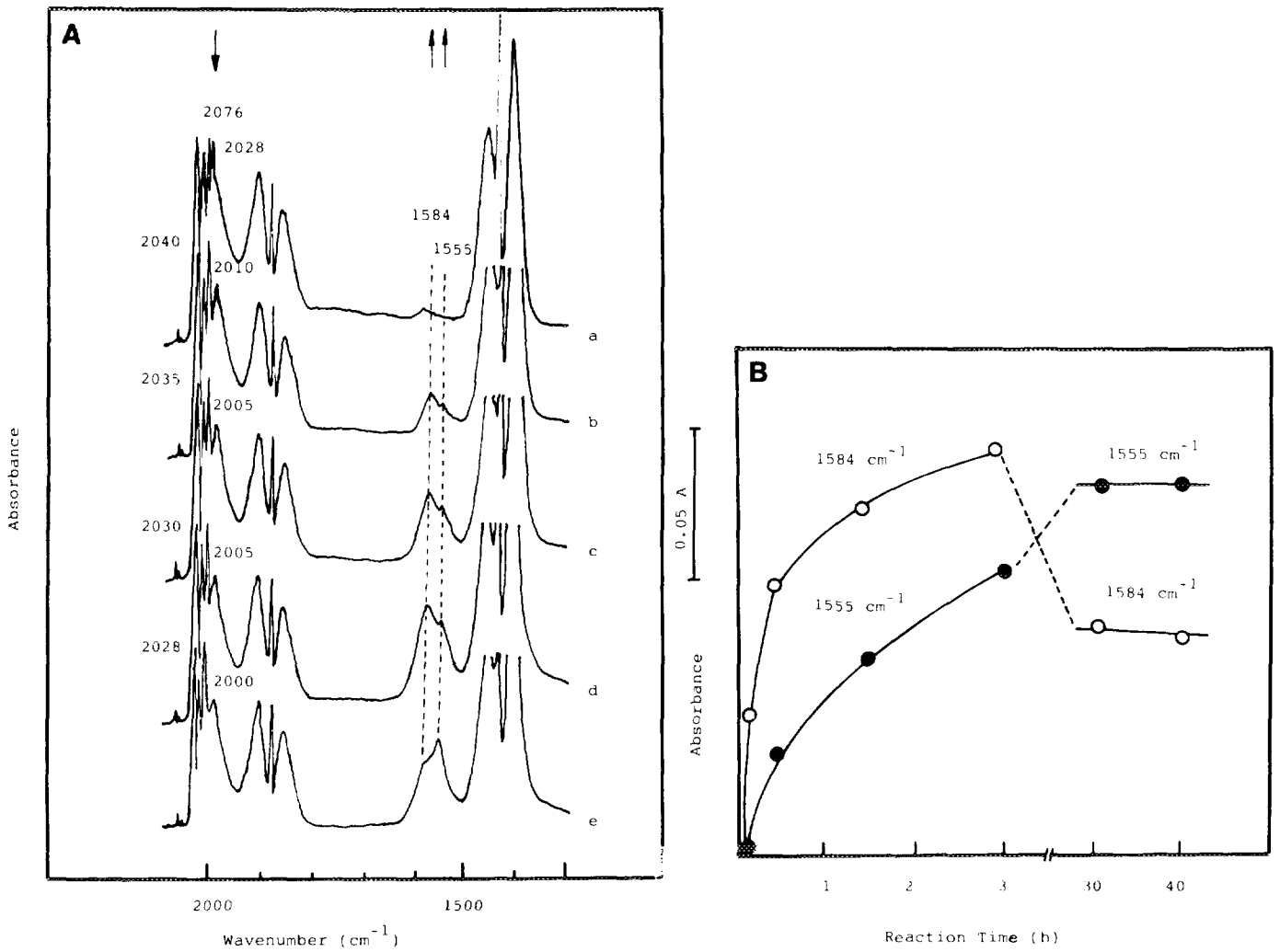

FIG. 11. (A) IR spectra of silica-supported reduced $Ru_3Co_3(CO)_{15}$ carbonyl cluster-derived catalyst after reaction with CO, H_2, and C_2H_4 (reaction flow: $H_2/CO/C_2H_4$ = 1/1/1, total 60 ml/min; reduction flow: H_2 40 ml/min) at various times. (a) The reaction for 30 min at 393 K; (b) after (a), reaction for 5 min at 443 K; (c) after (b), the reaction for 30 min at 443 K; (d) after (c), reaction for 3 h at 443 K; (e) after (d), reaction for 40 h at 443 K. (B) Plots of IR band intensity for 1584 and 1555 cm^{-1} bands versus reaction time over silica-supported reduced $Ru_3Co_3C(CO)_{15}$ carbonyl cluster-derived catalyst at reaction gas flow ($H_2/CO/C_2H_4$ = 1/1/1, total 60 ml/min) at 443 K.

lysts, and Ru–Co bimetallic carbonyl cluster-derived catalysts might be due to the promotion effect of Co atom in Ru–Co bimetallic carbonyl clusters. The Ru/Co bimetallic sites formed in Ru–Co bimetallic carbonyl cluster-derived catalysts appear to have a strong synergy effect for ethylene hydroformylation.

On the other hand, we clearly observed different catalytic behavior in the ethylene hydroformylation on SiO_2, carbon, and MgO supports. On silica- and carbon-supported Ru–Co bimetallic carbonyl cluster-derived catalysts, the activity and selectivity towards oxygenates are very high, in contrast to those on silica and carbon-supported $Ru_3(CO)_{12}$ and $Co_4(CO)_{12}$. This indicates a strong synergy effect of the Ru/Co bimetallic sites in ethylene hydroformylation. Comparatively, on MgO-supported Ru–Co bimetallic carbonyl clusters, the Ru/Co synergy effect is much lower. This may result from the nature of various supports. It is well known that MgO is a typical basic oxide (64). The basic oxides significantly affect the selectivity of products, which may reduce the effect of Ru/Co bimetallic sites. Ichikawa (47) reported catalytic hydroformylation of olefin over rhodium carbonyl cluster supported on SiO_2, Al_2O_3, MgO, and ZnO, and suggested that metal carbonyl clusters would be stabilized, and metal-carbonyl bonding would be strengthened in dispersion on basic oxides. Katzer *et al.* (65) studied the role of support in CO hydrogenation over supported rhodium and suggested that the more basic oxides have a higher Fermi level and thus have greater electron-donating capabilities. The above factors markedly influence activity and

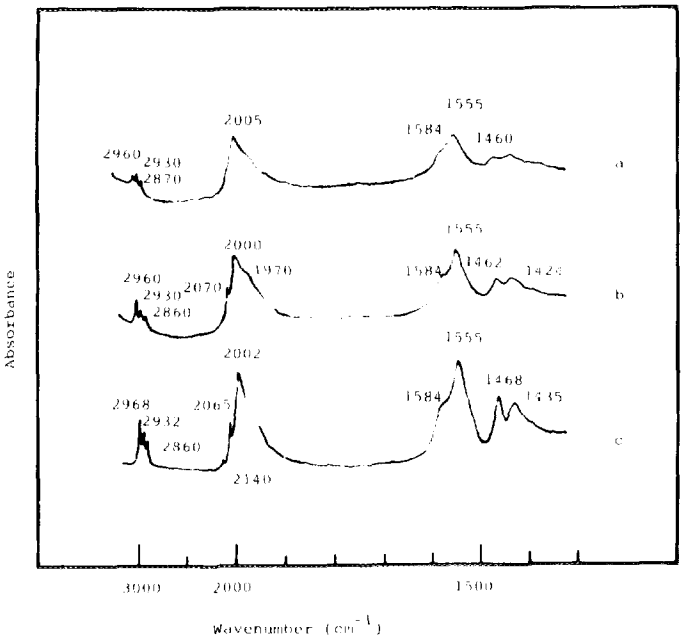

FIG. 12. IR spectra of the reduced (a) $H_3Ru_3Co(CO)_{12}$, (b) $Ru_3Co_3C(CO)_{15}$, and (c) $HRuCo_3(CO)_{12}$ carbonyl cluster-derived catalyst after reaction with H_2, CO, and C_2H_4 for 30 h at 443 K (reaction flow: $H_2/CO/C_2H_4$ = 1/1/1, total 60 ml/min; reduction flow: hydrogen 40 ml/min).

selectivity in ethylene hydroformylation. Additionally, we note that the MgO is an active support for ethylene hydroformylation, while silica and carbon are completely inactive. The IR spectra for CO + H_2 + C_2H_4 and CO + H_2 on MgO show bands at 1603, 1360, and 1340 cm^{-1} (66), which are reasonably assigned to formate species on the MgO surface (67). Relatively, we do not observe these bands in IR spectra for the adsorption of CO + H_2 + C_2H_4 and CO + H_2 on silica. Therefore, it is suggested that the surface formate may be the active species for the formation of propaldehyde and propanol in ethylene hydroformylation, in good agreement with the formation of oxygenates in CO hydrogenation suggested by Solymosi *et al.* (24–26).

Infrared Spectra

Relationship between IR bands and catalytic performance. Figures 9–12 and Table 5 show that there is a good correlation between the yields of propaldehyde and propanol in ethylene hydroformylation and the intensities of 1584 and 1555 cm^{-1} bands on the catalysts prepared from the different Ru–Co carbonyl clusters. The particular bands at 1584 and 1555 cm^{-1} were not observed on Ru_3/SiO_2, Ru_6C/SiO_2, Co_4/SiO_2, and even Ru_3 + Co_4/

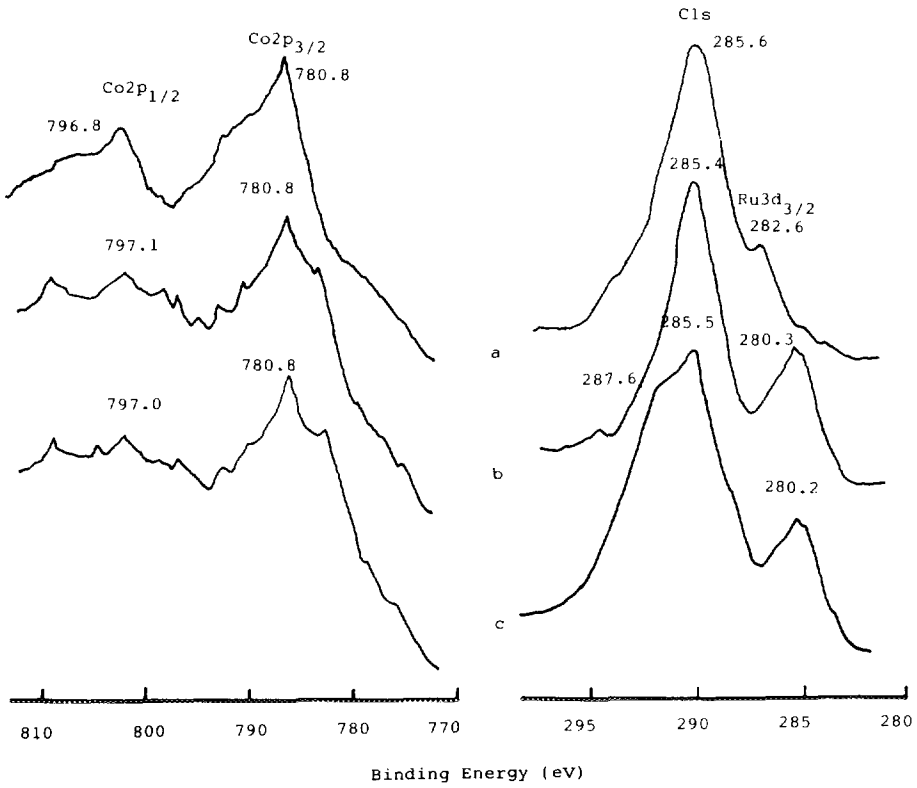

FIG. 13. The XPS spectra of Co3*p* and Ru3*d*. (a) Fresh silica-supported $HRuCo_3(CO)_{12}$ carbonyl cluster-derived catalyst; (b) the $RuCo_3/SiO_2$ catalyst was reduced for 2 h at 573 K; (c) after (b), the $RuCo_3/SiO_2$ catalyst was exposed to the mixture gases of CO, H_2, and C_2H_4 ($H_2/CO/C_2H_4$ = 1/1/1, total 60 ml/min) for 30 h at 443 K.

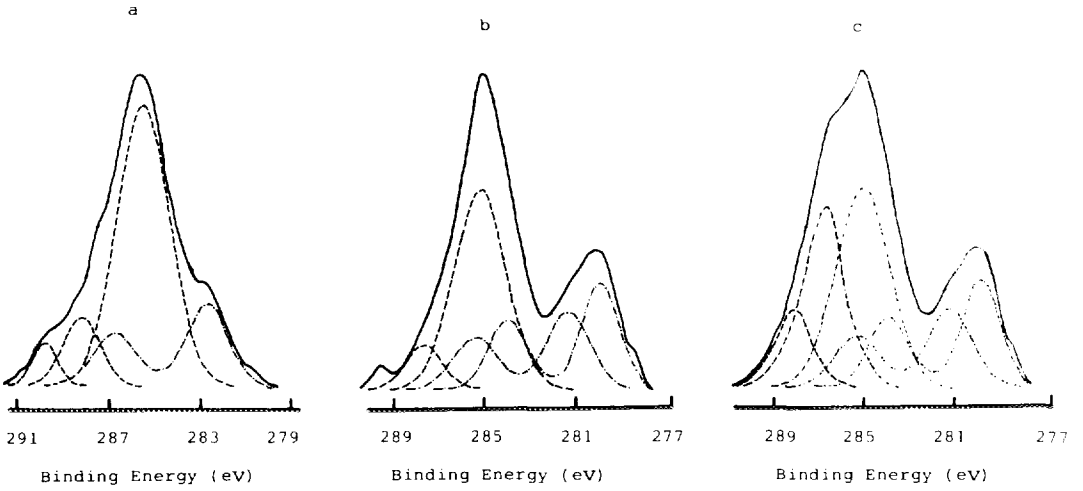

FIG. 14. The fitting C1*s* and Ru3*d* spectra by computer. (a) Fresh silica-supported $HRuCo_3(CO)_{12}$ carbonyl cluster-derived catalyst; (b) the $RuCo_3SiO_2$ catalyst was reduced for 2 h at 573 K; (c) after (b), the $RuCo_3/SiO_2$ catalyst was exposed to the mixture gases of CO, H_2, and C_2H_4 ($H_2/CO/C_2H_4$ = 1/1/1, total 60 ml/min) for 30 h at 443 K.

SiO_2 catalysts under the same reaction conditions. On the other hand, we observed no linear relationship between activity of propaldehyde and propanol in ethylene hydroformylation and the intensity of the 2000 cm^{-1} band formed in ethylene hydroformylation. Moreover, as observed in Fig.11, increasing the reaction time leads to the increase of the 1555 cm^{-1} species, while the 1584 cm^{-1} species decreases considerably. The formation of the 1555 cm^{-1} species, may be explained by two possibilities:(i) CO inserts in the ethyl adsorbed on the surface, forming the 1555 cm^{-1} species or (ii) the 1584 cm^{-1} species is converted into the 1555 cm^{-1} species by the reaction with adsorbed ethylene on the surface. By analysis of the above two possibilities, apparently the former is contrary to the experimental data. According to the former possibility, the intensity of 1584 cm^{-1} band could not be influenced by the formation of the 1555 cm^{-1} species. In fact, we observe that in the reaction time from 3 to 30 h or more than 30 h the intensity of 1584 cm^{-1} species decreased with reaction time, while the intensity of 1555 cm^{-1} band increased with reaction time considerably, indicating that the 1555 cm^{-1} species is derived from 1584 cm^{-1} species by the reaction with adsorbed ethylene. By the comparison of IR spectra and catalytic activity and selectivity for propaldehyde and propanol in ethylene hydroformylation, it is suggested that the propaldehyde and propanol are directly formed by the hydrogenation of the 1555 cm^{-1} species, and the 1555 cm^{-1} species is a possible intermediate for the formation of propaldehyde and propanol in ethylene hydroformylation.

Assignment of IR spectra in ethylene hydroformylation. The IR spectra in ethylene hydroformylation show the bands at 2960, 2880, 2070, 2000, 1971, 1584, 1555, and 1430 cm^{-1}. The bands at 2960–2860 and 1460–1420 cm^{-1} correspond to the C–H stretching and deformation frequencies, and the bands at 2080–1960 and 1880–1800 cm^{-1} are assigned to linear and bridging CO on the Ru surface, in agreement with previous work (9, 10, 29–33, 48, 49, 54, 68). The 1584 cm^{-1} species has been discussed by *Xias et al.* (9) recently, who suggested two possible structures, formate and formyl species, with the formyl being more likely than the formate species.

The assignment of 1555 cm^{-1} species formed in ethylene hydroformylation over the Ru–Co bimetallic carbonyl cluster-derived catalysts is likely to be the propionyl group adsorbed on the Ru–Co bimetallic sites, as shown in Fig. 15. The main reasons for this are: (i) The 1555 cm^{-1} species results from the reaction of 1584 cm^{-1} species with adsorbed ethylene group (Fig. 11); (ii) the adsorption of both propaldehyde and propanol exhibits the 1555 cm^{-1} bands (Fig. 7); (iii) The adsorption of D-labeled CH_3CDO gives rise to 1557 cm^{-1} bands (Fig. 8), which indicates that the CH_3CO group adsorbs on the Ru/Co bimetallic sites in Ru–Co carbonyl cluster-derived catalysts, and there is no C–D species on the surface of the catalysts. Furthermore, this result also indicates that the CH_3CO group is more stable than HCO adsorbed on the Ru/Co

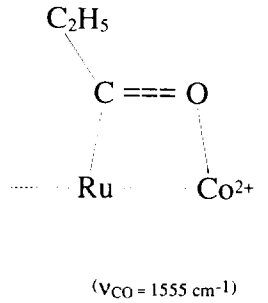

FIG. 15. The proposed model of 1555 cm^{-1} species formed in ethylene hydroformylation over silica-supported Ru–Co bimetallic carbonyl cluster-derived catalysts.

bimetallic sites in the catalysts, and it is possible for the 1584 cm^{-1} species to convert into 1555 cm^{-1} group; (iv) the reaction of $CO + H_2 + C_2H_4$, $^{13}CO + H_2 + C_2H_4$, and $^{13}CO + D_2 + C_2H_4$ at 443 K exhibit bands at 1555, 1520, and 1519 cm^{-1}, respectively (66), which are the same as the results (69) calculated by the theoretical models; (v) such low carbonyl stretching frequencies (1520–1580 cm^{-1}) of the acyl group have also been observed in $H_2Ru_3(CO)_9CHCH_3CO$ (45) and $Mn(CH_3)(CO)_5$ (53), as reported by Shriver and co-workers; (vi) the acyl species have been suggested as the intermediates for the formation of oxygenates in CO hydrogenation (9, 21, 22) and hydroformylation of olefin (14, 70).

The Possible Mechanism for Oxygenated Compounds in Ethylene Hydroformylation

The possible mechanism of formation of propaldehyde and propanol in ethylene hydroformylation over Ru–Co bimetallic carbonyl cluster-derived catalysts is proposed in the following steps: (i) The adsorption of CO, H_2, and ethylene on the surface of Ru sites occurs; (ii) the hydrogenation of adsorbed ethylene gives adsorbed ethyl group, which is further hydrogenated to ethane; (iii) CO inserts into adsorbed hydrogen to form the formyl species bound to Ru/Co bimetallic sites; (iv) the 1584 cm^{-1} species reacts with adsorbed ethylene to give propionyl group, appearing at 1555 cm^{-1} band in the IR spectra; (v) the hydrogenation of propionyl group results in the formation of propaldehyde, and further hydrogenation of adsorbed propaldehyde gives propanol.

CONCLUSION

The important conclusion of this study may be summarized as follows:

(i) The activity and selectivity for propaldehyde and propanol in ethylene hydroformylation on a series of Ru–Co bimetallic carbonyl cluster-derived catalysts are very high, in contrast to those on supported $Ru_3(CO)_{12}$, $Ru_6C(C)_{17}$, and $Co_4(CO)_{12}$ cluster-derived catalyst.

(ii) The Ru–Mn bimetallic carbonyl cluster-derived catalyst shows similar conversion, but poor activity and selectivity for oxygenates in ethylene hydroformylation, and the Cr_2Ru_3/SiO_2 catalyst exhibits very low activity and selectivity for both ethane and oxygenates in ethylene hydroformylation, as compared with the Ru_6C/SiO_2 catalyst.

(iii) The nature of supports has been shown to have a large influence on the catalytic activity and selectivity of the resulting catalyst. The effect of CO promotion in Ru–Co carbonyl clusters on silica and carbon is stronger than that on MgO.

(iv) The IR spectra of $CO + H_2 + C_2H_4$ on Ru–Co bimetallic carbonyl cluster-derived catalysts reveal that the intensity of the bands at 1584 and 1555 cm^{-1} have a good linear correlation with the activity for oxygenates in ethylene hydroformylation.

(v) With increasing reaction time, the 1584 cm^{-1} species can be converted into 1555 cm^{-1} species by reaction with adsorbed ethylene group on the surface. The 1555 cm^{-1} species are tentatively assigned to the carbonyl frequency of propionyl group adsorbed on Ru/Co bimetallic sites in Ru–Co carbonyl cluster-derived catalysts. The hydrogenation of 1555 cm^{-1} species gives propaldehyde, and the further hydrogenation of adsorbed propaldehyde produces propanol.

(vi) The Co2*p* and Ru3*d* spectra of reduced and used $RuCo_3/SiO_2$ catalysts show that the Co sites are in chemical states Co^{2+}, and that there are two types of Ru sites, giving chemical states of Ru^0 and $Ru^{\delta+}$ ($\delta = 0$–1).

ACKNOWLEDGMENTS

This work was supported by the National Natural Science Foundation of China and the Japan–US Cooperative Science Program. We thank Professor D. F. Shriver for the help of synthesizing some clusters.

REFERENCES

1. Gates, B. C., Guczi, L., and Konzinger, H. (Eds.), "Metal Cluster in Catalysis." Elsevier, Amsterdam, 1986.
2. Basset, J. M., Gates, B. C., Candy, J. P., Choplin, A., Leconte, M., Quignard, F., and Santini, C. (Eds.), "Surface Organometallic Chemistry: Molecular Approaches to Surface Catalysis." Kluwer Academic, Dordrecht, 1988.
3. Yermakov, Y. I., Kuznetsov, B. N., and Zakharov, V. A., "Catalysis by Supported Complexes." Elsevier, Amsterdam, 1981.
4. Basset, J. M., and Ugo, R., *in* "Aspects of Homogeneous Catalysis" (R. Ugo, Ed.), Vol. 3, p. 127. Reidel, Dordrecht, 1977.
5. Ichikawa, M., *in* "Tailored Metal Catalysts" (Y. Iwasawa, Ed.), p. 183. Reidel, Dordrecht, 1986.
6. Yokoyama, T., Yamazaki, K., Kosugi, N., Kuroda, H., Ichikawa, and Fukushima, T., *J. Chem. Soc., Chem. Commun.*, 962 (1984).
7. Ichikawa, M., *Polyhedron* **7**, 2351 (1988).
8. Choplin, A., Huang, L., Theolier, A., Gallezot, P., Basset, J. M., Siriwardane, U., Shore, S. G., and Mathieu, R., *J. Am. Chem. Soc.* **108**, 4224 (1986).
9. Xiao, F.-S., Fukuoka, A., and Ichikawa, M., *J. Catal.* **138**,206 (1992).
10. Xiao, F.-S., Fukuoka, A., Ichikawa, M., Henderson, W., and Shriver, D. F., *Catal. Lett.* **6**, 361 (1990).
11. Fukushima, T., Arakawa, K., and Ichikawa, M., *J. Phys. Chem.* **89**, 4440 (1985).
12. Fukushima, T., Araki, K., and Ichikawa, M., *J. Chem. Soc., Chem. Commun.*, 148 (1986).
13. Fukuoka, A., Rao, L.-F., and Ichikawa, M., *Catal. Today* **6**, 55 (1989).
14. Fukuoka, A., Kimura, T., Kosugi, N., Kuroda, H., Minai, Y., Sakai, Y., Tominaga, T., and Ichikawa, M., *J. Catal.***126**, 434 (1990).
15. Wentrcek, P. R., Wood, B. J., and Wise, H., *J. Catal.* **43**, 363 (1976).

16. Araki, M., and Ponec, V., *J. Catal.* **44,** 439 (1976).
17. Sachtler, J. W. A., Kool, J. M., and Ponec, V., *J. Catal.* **56,** 284 (1979).
18. Biloen, P., Helle, J. N., and Sachtler, W. M. H., *J. Catal.* **58,** 95 (1979).
19. Cant, N. W., and Bell, A. T., *J. Catal.* **73,** 257 (1982).
20. Orita, H., Narita, S., and Tamaru, K., *J. Chem. Soc., Chem. Commun.*, 150 (1984).
21. Fukushima, T., Arakawa, H., and Ichikawa, M., *J. Chem. Soc., Chem. Commun.*, 730 (1985).
22. Ichikawa, M., and Fukushima, T., *J. Phys. Chem.* **89,** 1564 (1985).
23. Takeuchi, A., and Katzer, J. R., *J. Phys. Chem.* **86,** 2438 (1982).
24. Solymosi, F., Erdohelyi, A., and Kocsis, M., *J. Catal.* **75,** 219 (1982).
25. Solymosi, F., Erdohelyi, A., and Bansagi, T., *J. Catal.* **68,** 371 (1981).
26. Solymosi, F., Erdohelyi, A., and Kocsis, M., *J. Catal.* **65,** 428 (1980).
27. Datta Betta, R. A., and Shelef, M., *J. Catal.* **48,** 48 (1977).
28. Amenomiya, Y., *J. Catal.* **57,** 64 (1979).
29. Xiao, F.-S., Ichikawa, M., and Guo, X.-X., *Bull. Sci. (Zagreb)* **36,** 960 (1991). [in Chinese]
30. Ichikawa, M., Xiao, F.-S., Magpanty, C. G., Fukuoka, A., Henderson, W., and Shriver, D. F., *in* "Proceedings, Natural Gas Conversion Synthesis Symposium." Oslo, Aug. 12–17, 1990.
31. Ichikawa, M., Xiao, F.-S., Magpanty, C. G., Fukuoka, A., Henderson, W., and Shriver, D. F., *in* "Natural Gas Conversion" (A. Holmen, K.-J. Jens, and S. K. Lolboe, Eds.). Elsevier, Amsterdam, 1991.
32. Xiao, F.-S., Ichikawa, M., Magpanty, C. G., Fukuoka, A., Henderson, W., and Shriver, D. F., *in* "Proceedings, 7th Symposium on the Relation between Homogeneous and Heterogeneous Catalysis." Tokyo, May 17–21, 1992.
33. Xiao, F.-S., Ichikawa, M., Magpanty, C. G., Fukuoka, A., Henderson, W., and Shriver, D. F., *J. Mol. Catal.* **74,** 379 (1992).
34. Watson, P. R., and Somorjai, G. A., *J. Catal.* **72,** 347 (1981).
35. Sachtler, W. M. H., and Ichikawa, M., *J. Phys. Chem.* **90,** 4752 (1986).
36. Chuang, S. C., Tian, Y. H., Goodwin, J. G., Jr., and Wender, I., *J. Catal.* **96,** 396 (1985).
37. Jordan, D. S., and Bell, A. T., *J. Phys. Chem.* **90,** 4796 (1986).
38. Pino, P., Piacenti, F., and Bianchi, M., "Organic Synthesis via Metal Carbonyls" (I. Wender, P. Pino, Eds), p. 47. Wiley, New York, 1977.
39. Hadai, M., Fukuoka, A., Koyasu, Y., and Uchida, Y., *J. Chem. Soc., Chem. Commun.*, 516 (1984).
40. Hadai, M., Fukuoka, A., Koyasu, Y., and Uchida, Y., *J. Mol. Catal.* **35,** 29 (1986).
41. Jensen, M. P., Henderson, W., Johnson, D. H., Sabat, M., and Shriver, D. F., *J. Organomet. Chem.* **394,** 121 (1990).
42. Johnson, B. F. G., Lewis, J., Raithby, P. R., and Suss, G., *J. Chem. Soc., Dalton Trans.*, 1356 (1976).
43. Steinhart, P. C., Glandfelter, W. L., Hanley, A. D., Fox, J. R., and Geoffroy, G. L., *Inorg. Chem.* **19,** 332 (1980).
44. Hidai, M., Fukuoka, A., Koyasu, Y., and Uchida, Y., *J. Chem. Soc., Chem. Commun.*, 516 (1984).
45. Sailor, M. J., Brock, C. P., and Shriver, D. F., *J. Am. Chem. Soc.* **109,** 6015 (1987).
46. Ichikawa, M., *J. Catal.* **56,** 127 (1979).
47. Ichikawa, M., *J. Catal.* **59,** 67 (1979).
48. Brown, M. F., and Genzalez, R. D., *J. Phys. Chem.* **80,** 1731 (1980).
49. Kuznetsov, V. L., Bell, A. T., and Yermakov, *J. Catal.* **65,** 374 (1980).
50. Kawai, M., Uda, M., and Ichikawa, M., *J. Phys. Chem.* **89,** 1654 (1985).
51. Fukuoka, A., Rao, L.-F., and Ichikawa, M., *Chem. Soc. Jpn.*, 561 (1989).
52. Hoffman, F. M., Depola, R. A., *Chem. Phys. Lett.* **106,** 83 (1984).
53. Horwiz, C. P., and Shriver, D. F., *Adv. Organomet.* **23,** 219 (1984).
54. Little, L. H., *in* "Infrared Spectra of Adsorbed Species." Academic Press, New York, 1966.
55. Luchesi, P. L. J., and Carter, J. L., *J. Phys. Chem.* **66,** 1451 (1962).
56. Zhou, X., and Gulari, E., *Langmuir* **4,** 1332 (1988).
57. Kim, K. S., *Phys. Rev. B* **11,** 2177 (1975).
58. Folksson, B., *Acta Chem. Scand.* **27,** 287 (1973).
59. Chln, R. L., and Hercules, D., *J. Phys. Chem.* **86,** 360 (1982).
60. Hems, C. R., and Sinfelt, J. H., *Surf. Sci.* **72,** 229 (1978).
61. Ding, Y.-J., Doctoral dissertation, Dalian Institute of Chemical Physics, Chinese Academy of Sciences, Dalian, China.
62. Yokomiza, G. H., Louis, C., and Bell, A. T., *J. Catal.* **120,** 1 (1989).
63. Solymosi, F., and Pasko, J., *J. Catal.* **115,** 107 (1989).
64. Tanabe, K., "Solid Acid and Bases," Chaps. 3–5. Kodansha, Tokyo–Academic Press, New York, 1970; Tanabe, K., Misono, M., Ono, Y., and Hattori, T., "New Solid Acids and Bases Their Catalytic Properties." Kodansha, Tokyo, 1989.
65. Katzer, J. R., Sleight, A. R., Gajardo, P., Michel, J. B., Gleason, E. F., and McMillan, S., *Faraday Discuss. Chem. Soc.* **72,** 120 (1981).
66. Xiao, F.-S., unpublished results.
67. Kikuzono, Y., Kagami, S., Naito, S., Onishi, T., and Tamaru, K., *Faraday Discuss. Chem. Soc.* **72,** 135 (1981).
68. Luchesi, P. J., Cater, J. L., and Yates, D. J. C., *J. Phys. Chem.* **66,** 1452 (1962).
69. Pinchas, S., and Laulicht, I., *in* "Infrared Spectra of Labeled Compounds." Academic Press, New York, 1971.
70. Fukuoka, A., Matsuzaka, H., Hidai, M., and Ichikawa, M., *Chem. Lett.*, 941 (1987).